Molecular Mechanism of H^+ Conduction in the Single-File Water Chain of the Gramicidin Channel

Régis Pomès* and Benoît Roux†

*Structural Biology and Biochemistry, Hospital for Sick Children, and Department of Biochemistry, University of Toronto, Toronto, Ontario M5G 1X8, Canada; and †Biochemistry Department, Weill Medical College of Cornell University, New York, New York 10021 USA

ABSTRACT The conduction of protons in the hydrogen-bonded chain of water molecules (or "proton wire") embedded in the lumen of gramicidin A is studied with molecular dynamics free energy simulations. The process may be described as a "hop-and-turn" or Grotthuss mechanism involving the chemical exchange (hop) of hydrogen nuclei between hydrogen-bonded water molecules arranged in single file in the lumen of the pore, and the subsequent reorganization (turn) of the hydrogen-bonded network. Accordingly, the conduction cycle is modeled by two complementary steps corresponding respectively to the translocation 1) of an ionic defect (H^+) and 2) of a bonding defect along the hydrogen-bonded chain of water molecules in the pore interior. The molecular mechanism and the potential of mean force are analyzed for each of these two translocation steps. It is found that the mobility of protons in gramicidin A is essentially determined by the fine structure and the dynamic fluctuations of the hydrogen-bonded network. The translocation of H^+ is mediated by spontaneous (thermal) fluctuations in the relative positions of oxygen atoms in the wire. In this diffusive mechanism, a shallow free-energy well slightly favors the presence of the excess proton near the middle of the channel. In the absence of H^+, the water chain adopts either one of two polarized configurations, each of which corresponds to an oriented donor-acceptor hydrogen-bond pattern along the channel axis. Interconversion between these two conformations is an activated process that occurs through the sequential and directional reorientation of water molecules of the wire. The effect of hydrogen-bonding interactions between channel and water on proton translocation is analyzed from a comparison to the results obtained previously in a study of model nonpolar channels, in which such interactions were missing. Hydrogen-bond donation from water to the backbone carbonyl oxygen atoms lining the pore interior has a dual effect: it provides a coordination of water molecules well suited both to proton hydration and to high proton mobility, and it facilitates the slower reorientation or turn step of the Grotthuss mechanism by stabilizing intermediate configurations of the hydrogen-bonded network in which water molecules are in the process of flipping between their two preferred, polarized states. This mechanism offers a detailed molecular model for the rapid transport of protons in channels, in energy-transducing membrane proteins, and in enzymes.

INTRODUCTION

The control of proton fluxes across biomembranes constitutes one of the most complex and fundamental properties of living systems. To achieve biological energy conversion (bioenergetics), membrane-spanning protein assemblies use energy provided by photochemical or redox reactions to pump protons against an electrochemical gradient, $\Delta\mu_{H+}$. In turn, the flow of H^+ in the direction of the electrochemical gradient drives ATP synthesis (Saraste, 1999). This "chemiosmotic coupling" is the cornerstone of bioenergetics (Mitchell, 1961). Despite the importance of proton transport phenomena, detailed molecular mechanisms have remained elusive. A high level of detail is required to understand proton-pumping mechanisms (Wikström, 1998; Sjogren et al., 2000; Lanyi, 2000). In general, it is particularly challenging to understand the forces driving proton movement in enzymes, because it requires knowledge, at the atomic level, of three equilibrium properties that are intimately coupled to each other: 1) the protonation state of all titratable groups in the protein; 2) the electronic (charge) state of the protein; and 3) the equilibrium distribution of conformational states of the enzyme. Furthermore, these properties must be characterized at each stage of the catalytic cycle. This is a formidable undertaking for the complex membrane-bound protein assemblies involved in energy transduction and/or proton pumping, as illustrated in the cases of bacteriorhodospin, a light-driven proton pump (Lanyi, 1999), of bacterial photosynthetic reaction centers (Okamura et al., 2000), and of cytochrome *c* oxidase, a redox-coupled proton pump (Zaslavsky and Gennis, 2000).

In addition to these equilibrium properties, the structure and function of well-defined pathways for proton translocation, without which leaks resulting in the loss of proton activity would occur, must be elucidated. The transient events (nonequilibrium properties) involved in proton movement present a special challenge in their own right. Unlike that of other ions, the transport of protons does not require the net diffusion of atomic or molecular species, but may instead take place according to a Grotthuss relay mechanism involving the chemical exchange of hydrogen nuclei along successive hydrogen-bond donor and acceptor groups forming extensive networks and the subsequent reorganization of these networks (Grotthuss, 1806; Nagle and Morowitz, 1978; Knapp et al., 1980; Agmon, 1995) (Fig. 1). Such

Submitted August 14, 2001, and accepted for publication January 22, 2002.

Address reprint requests to Dr. Régis Pomès, Structural Biology & Biochemistry, Hospital for Sick Children, 555 University Avenue, Toronto, Ontario M5G 1X8, Canada. Tel.: 416-813-5686; Fax: 416-813-5022; E-mail: pomes@sickkids.ca.

0006-3495/02/05/2304/13 $2.00

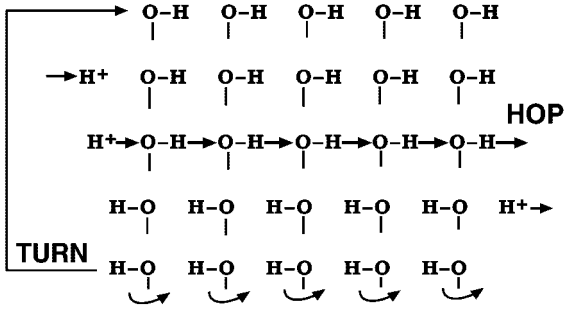

FIGURE 1 Schematic depiction of the hop-and-turn or Grotthuss mechanism for H^+ transport in a proton wire containing water and/or hydroxyde groups. A succession of proton-exchange ("hop") steps along a polarized hydrogen-bonded chain results in the translocation of an ionic defect, H^+, from end to end. This relay process leaves the chain in the opposite orientation, so that inversion of the chain ("turn") must take place to complete the translocation cycle. This latter process involves the directional migration of a bonding defect triggered by the reorientation of each hydrogen-bearing group in the chain.

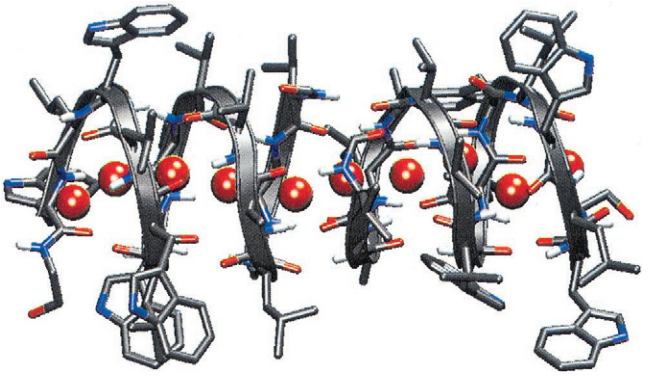

FIGURE 2 β-helix structure of the gA dimer. The narrow cylindrical pore is lined with peptide bonds and accommodates a single-file water chain of water molecules, depicted here as red spheres. This picture was generated with the VMD software (Humphrey et al., 1996).

pathways constitute "proton wires" mediating H^+ displacement over long distances.

Although the molecular structures of such important proton pumps as bacteriorhodopsin and cytochrome *c* oxidase are known, the detailed nature of proton pathways and the molecular mechanisms leading to proton translocation are still unclear. In addition to proton-relaying amino acid residues, energy-transducing proteins, like ion channels, appear to use water wires. Models for the relay of H^+ by buried water molecules have been substantiated in several systems of bioenergetic interest. In particular, there is now abundant evidence for the involvement of buried water molecules in bacteriorhodopsin (for recent reviews, see Dencher et al., 2000; Luecke, 2000; Kandori, 2000). However, high-resolution structures of intermediates in the pumping cycle suggest that although several water molecules reside in the protein interior, they may not at all times form a continuous hydrogen-bonded chain (Lanyi, 2000). Thus, water wires make up extended but incomplete tracts of the proposed H^+ pathways, underlining the importance of conformational changes and dynamic fluctuations in proton transport. This, in turn, raises further questions: do water chains function as passive units, or are they involved in the controlled access, blockage, and gating of proton flow? Understanding the properties governing proton transport in hydrogen-bonded networks containing water molecules is a prerequisite to achieving full description of both ion permeation and energy-transduction mechanisms. To this end, the study of simple proton wires can help in characterizing the fundamental principles governing proton translocation.

Gramicidin constitutes a model of choice for the study of proton conduction in much more complex proteins (Quigley et al., 1999; Cukierman, 2000; DeCoursey and Cherny, 1999). With the notable exception provided by the potassium channel KcsA (Doyle et al., 1998), it is to this day the only ion channel for which detailed structure-function relationships have been characterized, both experimentally (Tian and Cross, 1999) and theoretically (Roux and Karplus, 1994). The relative structural and functional simplicity of gramicidin A (gA) permits one to approach the proton transport mechanism "in isolation." In its active form, gA assembles as a head-to-head homodimer of pentadecapeptides in lipid bilayers (Arseniev et al., 1985). Its alternating L- and D-amino acids adopt a right-handed $\beta^{6.3}$-helix structure, which leaves its hydrophobic side chains facing out into the bilayer and its peptide backbone lining the interior of a cylindrical pore 4 Å in diameter (Fig. 2). This hydrophilic pore accommodates a single file of water molecules and mediates the translocation of monovalent cations such as H^+, Cs^+, Na^+, and K^+ (Finkelstein, 1987). The partial dehydration of cations upon entry into the single-file region is partly compensated by the channel backbone. Whereas permeation of other ions necessitates the net diffusion of the single-file water column, the absence of streaming potentials during H^+ permeation through gramicidin (Levitt et al., 1978) indicates that the long-range translocation of H^+ arises from a Grotthuss mechanism (Akeson and Deamer, 1991).

In recent years, theoretical studies of proton transport by hydrogen-bonded networks of water molecules have opened the way to the study of biological proton wires. The molecular basis for the hop-and-turn mechanism has been investigated in bulk water (Tuckerman et al., 1995; Vuillemier and Borgis, 1998, 1999; Schmitt and Voth, 1999), in single-file water chains or "water wires" embedded in model channels (Pomès and Roux, 1995, 1996a, 1998; Pomès, 1999; Drukker et al., 1998; Decornez et al., 1999; Mei et al., 1998; Sadeghi and Cheng, 1999; Brewer et al., 2001), and in gA (Pomès and Roux, 1996b; Sagnella et al., 1996). These studies have uncovered important aspects of the hop and turn mechanism at the molecular level. In particular, the respective roles of thermal fluctuations and of nuclear quan-

tum effects arising form the light mass of H^+, and the modulation of proton-transport properties by a protein matrix have been explored in simple, yet biologically-relevant systems.

The Grotthuss mechanism in protonated chains of water molecules forming a linear hydrogen-bonded array in nonpolar channels was the object of several computational studies (Pomès and Roux, 1995, 1996a, 1998; Pomès, 1999; Drukker et al., 1998; Decornez et al., 1999; Mei et al., 1998; Sadeghi and Cheng, 1999; Brewer et al., 2001). The hopping of H^+ was found to be dominated by structural fluctuations modulating donor-acceptor separations in the hydrogen-bonded chain that take place spontaneously at 300 K. These fluctuations drive the exchange between OH_3^+-like and $O_2H_5^+$-like species (Pomès and Roux, 1995). The translocation of protons across several water molecules may occur in subpicosecond time scales (Pomès and Roux, 1996a; Sadeghi and Cheng, 1999). Nuclear quantum effects (zero-point energy and quantum tunneling of hydrogen nuclei) on the equilibrium structure of hydrogen-bonded chains of water molecules have been studied with discretized Feynman path integral for the treatment of exchanging protons. These effects, although significant, do not govern the transfer process in equilibrium conditions (Pomès and Roux, 1995, 1996a; Mei et al., 1998; Brewer et al., 2001). By contrast, under nonequilibrium initial conditions mimicking the effect of an external electric field (Drukker et al., 1998) and of hydrogen-bonding partners restricting the displacements of water molecules (Decornez et al., 1999), nuclear tunneling and nonadiabatic transitions may play an important role in the translocation.

Studies of bulk water (Tuckerman et al., 1995) and gramicidin (Pomès and Roux, 1996b) have revealed how structural fluctuations of the hydrogen-bonded network fundamentally dominate the rapid, passive relay of H^+. More specifically, changes in the hydrogen-bond connectivity of water molecules control the progress of ionic translocation in these systems. In bulk water, such changes consist of making and breaking hydrogen bonds in the second hydration shell of H^+. In gA, proton hopping appears to be limited by the migration of defects in the polarization of the wire. These defects result from hydrogen bond interactions between water molecules and carbonyl oxygen atoms lining the pore interior. Accordingly, comparisons between the proton translocation mechanism in gA and in model hydrophobic pores suggest that the Grotthuss mechanism is highly sensitive to the detail of hydrogen-bonding and electrostatic interactions between the water wire and the channel (Pomès and Roux, 1996b; Pomès, 1999). Finally, calculations of the free energy or potential of mean force (PMF) for both hop and turn steps of the Grotthuss mechanism in nonpolar channels indicated that the reorientation of the wire, unlike hopping, is a thermally activated process (Pomès and Roux, 1998), suggesting that the reorganization of the wire, not the passage of H^+ itself, limits the rate of proton translocation in these simplified models.

In this article, the molecular mechanism governing both ionic and bonding translocation steps in gA is investigated. The molecular dynamics and free energy simulation approaches used previously are applied to the chain of water molecules embedded in gA. The structure, dynamic fluctuations, and thermodynamic properties of the hydrogen-bonded network formed by the water molecules are computed successively with and without an excess proton. The present study focuses on the effect of the gramicidin channel on proton conduction. To this end, a detailed analysis of the hop and turn process is presented and compared with the results obtained previously in nonpolar channels.

MATERIALS AND METHODS

Molecular model

The molecular model used in the molecular dynamics simulations described below consists of the head-to-head pentadecapeptide dimer forming the gA pore, together with water molecules. The system contains three well-defined sections: the polypeptidic dimer, the single-file water chain, and two cylindrical caps of water molecules lying outside the mouths of the channel. The three-dimensional structure of gA has been determined from solid-state nuclear magnetic resonance spectroscopy (Arseniev et al., 1985; Ketchem et al., 1997) (Fig. 2). The starting configuration of the channel was taken from previous molecular dynamics simulations in which the lipid membrane was modeled explicitly (Woolf and Roux, 1994). As in previous simulations (Pomès and Roux, 1996b), harmonic restraining potentials (with a force constant of 0.1 kcal/mol/Å^2) were imposed on the heavy atoms of the eight Trp indole rings to preserve the overall fold of the pore without affecting directly the dynamics fluctuations of backbone atoms lining the pore interior. This constraint should be viewed as an approximation of the restriction to indole mobility due to interactions with the lipid membrane, which act as "anchors" of the indole rings (Woolf and Roux, 1994). In addition, harmonic constraints with the same force constant were also imposed on the heavy atoms of the peptide backbone during high-temperature preparation of the unprotonated wire (see below) to ensure conservation of the secondary structure of the pore.

The CHARMM force field, version 22 (Brooks et al., 1983; MacKerell et al., 1998), was used to model protein-protein interactions. The 10 water molecules, or proton wire, contained in the gA pore region, were modeled with the PM6 force field of Stillinger and coworkers (Stillinger and David, 1978; Stillinger, 1979; Weber and Stillinger, 1982). PM6 is a polarizable and dissociable model of water that consists of O^{2-} and H^+ moieties. It has been used in several previous studies of proton wires (Pomès and Roux, 1995, 1996a,b, 1998; Drukker et al., 1998; Decornez et al., 1999). This empirical force field reproduces relevant properties of protonated water chains (Pomès and Roux, 1996a) and has been shown, in a comparison with results obtained from ab initio simulations, to capture the essential features of the mechanism of H^+ transport in these systems (Mei et al., 1998). The parameters used to model PM6-peptide interactions are described elsewhere (Pomès and Roux, 1996b).

The force fields used for the caps of water molecules lying outside the pore differed in the protonated and the unprotonated systems. In the latter case, 14 PM6 water molecules were used in each cap, whereas in the former case, the TIP3P force field (Jorgensen et al., 1983) was used to model caps of 36 water molecules each. The parameters governing PM6-TIP3P interactions are given elsewhere (Pomès and Roux, 1998). Such a hybrid model offers the advantage of low computational cost compared with an all-PM6 model and allows the inclusion of water caps sufficiently

large to avoid finite-size effects that would preclude proton diffusion from end to end of the single file (Pomès and Roux, 1998). Because the TIP3P model is not dissociable, the hybrid model eliminates the possibility of an escape of H^+ out of the channel during the course of the simulations. Control simulations of the nonprotonated wire indicated that the equilibrium conformations of the water chain and the hydrogen-bonding coordination of interfacial water molecules obtained with the hybrid model are consistent with those obtained with all-PM6 and all-TIP3P models.

The cylindrical caps of water molecules were carved from a periodic box of TIP3P water equilibrated in the bulk, and superimposed onto the outer turn of the gA monomers. The water molecules overlapping with heavy atoms of the peptide were deleted, and in all the subsequent simulations, the cap region was subjected to a boundary potential. In the unprotonated (14-PM6 caps) and protonated (36-TIP3P caps) systems, radial (cylindrical) restraints acted on the O atoms lying respectively further than 6.8 and 6.0 Å from the main axis of the channel, and planar constraints were imposed outside of the ranges $11.0 < z < 15.0$ and $11.5 < z < 20$ Å from the channel center. These restraining potentials were quadratic with a force constant of 20 kcal/mol/Å^2. The inner value of the planar constraint was chosen so as to avoid the artifact of water diffusion in the nonpolar region of the membrane around the outside of gA. Similarly, planar restraints acting outside the range $-11 < z < 11$ Å (with a force constant of 20 kcal/mol/Å^2) were imposed on the 10 water molecules inside the pore to prevent their diffusion into the caps. The location of these planar boundaries was chosen so as to minimize perturbations of the interactions between pore and cap water molecules, as determined from unbiased simulations. No cutoff was imposed on nonbonded interactions.

Molecular dynamics simulations

The CHARMM program (Brooks et al., 1983) was used to propagate the Langevin equation of motion. A friction coefficient of 5 ps^{-1} was applied to all heavy atoms in the system. After an initial equilibration, the molecular systems were subjected to successive cycles of umbrella sampling calculations comprising preparation, equilibration, and production. The preparation stage was necessary to overcome the relatively long relaxation times associated with the propagation of bonding defects in the gA channel, as observed in previous simulations (Pomès and Roux, 1996b). Uncorrelated configurations of the protonated wire were obtained from simulations in which the electrostatic interactions between channel and single-file atoms were turned off. This artificial procedure was seen to lead to the disappearance of bonding defects and to high mobility of the ionic defect (Pomès and Roux, 1996b). The nonpolar channel resulting from this procedure is similar to the model channels constructed with radial restraints on single-file chains of water molecules, whose properties were characterized in previous studies (Pomès and Roux, 1995, 1996a, 1998). In such systems, complete translocation events from end to end of the single-file region occur in the order of a few picoseconds so that it is easy to equilibrate ionic defects by imposing collective reaction coordinate constraints (Pomès and Roux, 1998) before turning electrostatic interactions back on for equilibration and data collection (production). Using this procedure helped to reach statistical convergence in the PMF calculation.

The collective reaction coordinates used to follow the progress of ionic and bonding defects in the pore are defined as

$$\mu_z = \sum_i q_i z_i \qquad (1)$$

in which the summation runs over all water atoms O and H inside the pore, with charges $q_O = -2e$ and $q_H = 1e$ and cartesian coordinates z_O and z_H. In the case of the unprotonated wire, μ_z corresponds to the z component of the total molecular dipole moment of the 10-pore water molecules, whereas in the presence of an excess proton μ_z/e is the position of the center of charge along the z axis. These reaction coordinates reflect the organization of the wire and offer the advantage of a continuous variable for translocation of both ionic and bonding defects throughout the length of the pore (Pomès and Roux, 1998). The detail of the methodology is described below successively for the unprotonated and protonated systems.

Unprotonated wire

The initial conformation of the (single-file) wire region was obtained by deleting the excess proton from a previously equilibrated protonated gA wire (Pomès and Roux, 1996b). The water molecules were subjected to energy minimization and thermalization (two 10-ps runs at 150 and 300 K), whereas the peptide was held fixed, and the procedure was repeated without fixing protein atoms. The subsequent equilibration consisted of a 60-ps simulation at 300 K, during which all single-file water-water hydrogen bonds pointed toward the same mouth of the channel (polarized configuration). The calculation of the free energy profile, or PMF for the reorientation of the wire (i.e., propagation of the bonding defect–see Scheme 1), was obtained from a series of six molecular dynamics simulations with umbrella sampling, whereby the reaction coordinate μ_z was constrained by a harmonic potential $V_i(\mu_z) = \frac{1}{2}k_\mu (\mu_z - \mu^0_{z,i})^2$, with a force constant of $k_\mu = 2$ kcal/mol/(e·Å)^2 and successive reference values of $\mu^0_{z,i} = 9$, 8, 6, 4, 2, and 0 e·Å.

For each window i, four cycles of production were generated using the following procedure. 1) For preparation, a 5-ps simulation was run at 400 K (with backbone harmonic constraints on the channel backbone to prevent unraveling of the β-helix). 2) For equilibration, a 5-ps simulation followed, with $T = 300$ K. 3) For production, the data were collected from an ensuing 20-ps simulation at 300 K. The preparation stage was required to ensure that several distinct local minima be sampled that correspond to a given value of μ^0_z. Given the long characteristic times of reorganization of the hydrogen-bonded network, which was inferred to be of the order of 100 ps from earlier simulations of the gA channel (Pomès and Roux, 1996b), much longer simulations would be required to reach statistical convergence at 300 K. The higher temperature used in the preparation stage enables a larger number of conformations to be sampled in the relatively short simulation times amenable to our PMF calculation. For each window in the umbrella sampling calculation, 32,000 configurations were obtained at 2.5-fs intervals from a total of 80 ps of simulations. These configurations were used in the computation of the PMF (see below). The calculations were repeated with TIP3P single-file water molecules (Jorgensen et al., 1983) to gauge the influence of the water model in the calculations, as in similar calculations performed on nonpolar channels (Pomès and Roux, 1998; Pomès, 1999).

Protonated wire

The starting configuration of the channel with protonated water wire was taken from a previous simulation (Pomès and Roux, 1996b). Two cylindrical caps of 36 water molecules lying outside the mouths of the channel were added to the system. The energy was minimized (300 steps of steepest descent) and the caps were briefly thermalized (5 ps, 300 K) with the rest of the system held fixed. Eight series of biased simulations or windows were then created, each with a quadratic restraint $V_i(\mu_z)$ differing by their reference $\mu^0_{z,i}$ (see previous subsection). The reference values in the successive windows were $\mu^0_{z,i} = -0.5$, 0, 0.5, 1, . . . , 2.5, and 3 e·Å. The latter value corresponds to wires in which the excess proton is located at the interface between bulk and single-file regions (Pomès and Roux, 1998).

For each of these eight windows, the simulation protocol consisted of four iterations of the following cycle. 1) For preparation of the protonated wire, a 300-step SD energy minimization was followed by 5-ps MD equilibration of the proton in the single-file water wire at 350 K with wire-channel electrostatic interactions turned off. 2) For equilibration of the channel, a 300-step SD minimization was followed by 25-ps MD at 300 K with full electrostatic interactions. 3) Production consisted of 50 ps of data collection at 300 K. This procedure ensured the generation of four

uncorrelated production cycles to improve configurational averaging. Production times of 200 ps were generated for each window, for a total of 2560 ps of simulations including preparation, equilibration, and production.

PMF calculations

The wire configurations produced in the simulations of protonated and unprotonated systems were used to calculate the PMF for ionic and bonding defect translocations, respectively. To this end, the weighted histogram analysis method (Kumar et al., 1992, Roux, 1995) was used as in similar calculations reported previously (Pomès and Roux, 1998). Statistical convergence of the PMF was verified by comparing the profiles obtained from various subsets of configurations.

RESULTS AND DISCUSSION

Unprotonated wire

Equilibrium structure

The gA channel is a narrow cylindrical pore filled with an array of water molecules arranged as a single file (Arseniev et al., 1985; Ketchem et al., 1997; Fig. 2). The pore water molecules form a hydrogen-bonded network comprising both water-water and water-channel hydrogen bonds (Roux and Karplus, 1994, references therein; Pomès and Roux, 1996b). A water molecule is considered to belong to the single file if 1) it makes at most two hydrogen bonds with other water molecules and 2) at least one of these two coordinating water molecules is itself a single-file water. Thus defined, the single-file region contains eight water molecules. In addition, two outlying water molecules form an interface with water molecules outside the pore. Each of the eight single-file water molecules is surrounded by two adjacent water molecules with which it can either donate or accept a hydrogen and carbonyl O atoms of the channel to which it can donate a hydrogen atom. The single-file water molecules do not in general accept hydrogen atoms from the channel, because backbone N—H bonds, which are involved in intramolecular hydrogen bonds defining the β-helix fold, do not deviate sufficiently from colinearity with the channel axis to point toward water O atoms in the lumen.

A representative conformation of the water chain is depicted in Fig. 3. Most water molecules in the wire adopt the following organization: donation of one H to a channel backbone carbonyl, donation of the other H to a neighboring water, and acceptance of one H from the other neighboring water, for a total of three hydrogen bonds. Such a coordination results in a continuous chain of water-water hydrogen bonds. In the single-file region, water O—H bonds involved in hydrogen bonding (donation) to the channel are approximately perpendicular to the channel axis, and most of the covalent O—H bonds making up the water-water hydrogen-bonded chain point toward the same entrance of the gA dimer: the hydrogen-bonded chain is preferentially polarized. The projection of the dipole moment of each of these water molecules along the z axis is approximately μ_{zi}

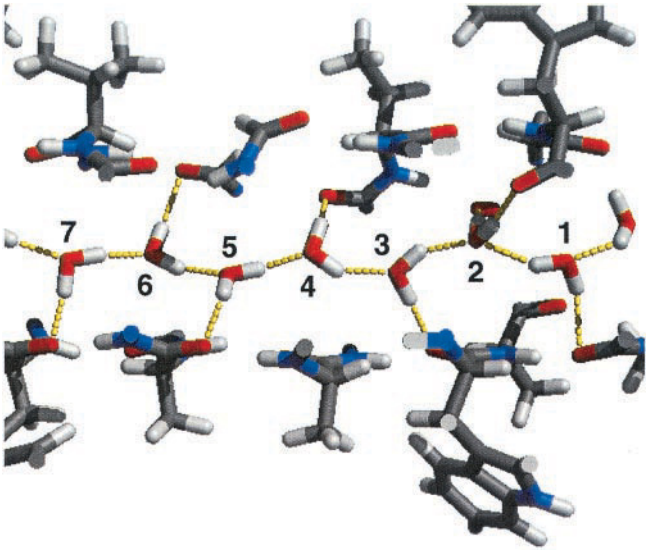

FIGURE 3 Representative structure of the hydrogen-bond network of water molecules inside gA without an excess proton. Seven of the 10 water molecules located inside the pore are shown. All of them are tricoordinated and donate one H atom to carbonyl O atoms of the channel, except for water 2, which is oriented perpendicularly to the channel axis and forms four hydrogen bonds, donating both of its H atoms to the channel. The polarization of water molecules inverts around water 2, which defines a bonding defect.

$\cong \pm 1$ e·Å. In addition to the polarized chain, in general the wire also contains exactly one water molecule that donates both of its H atoms to the channel. Such coordination forces the plane of that water molecule to be approximately perpendicular to the channel axis, with $\mu_{zi} \cong 0$. In general, the two water molecules adjacent to this perpendicular water point one of their O—H bonds toward it. The resulting inversion in the topology of the hydrogen-bonded network defines what we shall refer to as a bonding defect.

The average hydrogen-bonding coordination of each of the 10 water molecules in the wire was computed from a 20-ns simulation of the unprotonated wire with the TIP3P water model (Table 1). Results obtained from shorter simulations with the PM6 model (not shown) are highly similar. The asymmetry in the coordination of pairs of water molecules with indices i and $(11 - i)$ indicates that statistical convergence is not achieved within 20 ns. Nevertheless, this analysis underlines important features in the organization of the hydrogen-bonded network. The preferred arrangement of the wire is reflected in the dominance of a hydrogen-bonding coordination of three for the single-file water molecules (indices 2–9). The seemingly high occurrence of null H bond coordination between water and channel (12%) reflects the fact that a multiple choice of carbonyl O atoms often results in bifurcated H bonds, which are not counted. The bonding defect, characterized by donation of 2 H to the channel, is preferentially at water 2, 3, 8, or 9, near the end of the single file. This bonding defect is not necessarily a

TABLE 1 Hydrogen-bonding coordination* of pore water molecules averaged over a 20-ns MD simulation (in percentage points)

Water (#)	Water to channel			Water-water			Number of H bonds			
	0	1	2	1	2	3	1	2	3	4
1	9	85	5	11	47	42	1	10	45	44
2	8	58	34	25	75	0	2	19	58	21
3	11	71	19	19	81	0	2	19	67	12
4	11	86	3	11	89	0	2	17	79	2
5	16	82	2	9	91	0	2	20	76	2
6	19	79	1	12	88	0	2	24	71	2
7	12	86	2	14	86	0	2	20	75	2
8	14	77	9	16	84	0	2	21	70	7
9	13	71	16	17	83	0	2	21	67	10
10	9	88	3	8	48	44	1	9	45	45
Average	12	78	10	15†	85†	0†	2†	20†	70†	6†

*Assuming that a hydrogen bond is formed whenever the donor-acceptor separation is less than 3.2 Å and the donor-H-acceptor angle is greater than 120 degrees.

†Averages performed on the single-file water molecules (indices 2–9) only.

hydrogen-bonding defect: although water molecules 2, 3, 8, and 9 are more likely than the other single-file water molecules to be engaged in only one water-water bond, they are also more likely to form a total of four H bonds. However, even if the hydrogen-bonded chain is continuous, the local inversion of its polarity precludes passage of protons in the sense of a Grotthuss mechanism (see Fig. 1). Finally, interfacial water molecules (indices 1 and 10) often make two hydrogen bonds with outlying water molecules, preferably as acceptors. This preferred orientation reflects the presence of an intervening bonding defect.

The preferred organization of the unprotonated wire as a polarized water chain is not due to the gA channel, which, by virtue of its β-helical secondary structure and its assembly as a head-to-head homodimer, possesses no net dipole moment. Rather, the polarization is an intrinsic property of the single-file water chain, which was attributed to the maximization of favorable water dipole-dipole interactions in nonpolar channels (Pomès and Roux, 1998; Pomès, 1999). The presence of a bonding defect in the preferred conformations of the unprotonated water wire in gA contrasts with the fully polarized chains obtained in hydrophobic channel models. Full polarization is driven by the optimization of dipole-dipole interactions between the single-file water molecules. The preferred location of the bonding defect, near the end of the single file, maximizes the length of the polarized segment in gA.

Dynamic fluctuations

Pore water molecules can adopt three distinct polarization states corresponding respectively to $\mu_{zi} \cong +1, -1$ (polarized), and 0 e·Å (bonding defect). The reorientation of water molecules gives rise to unitary transitions between these

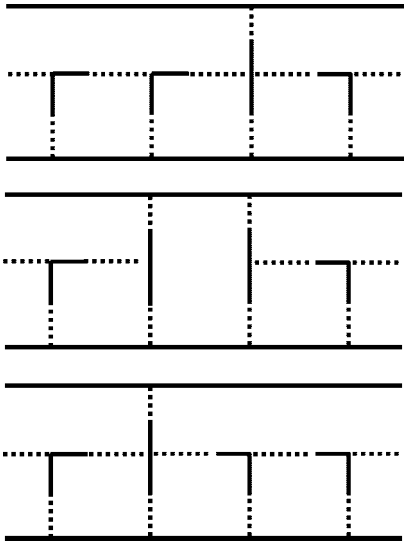

FIGURE 4 Schematic representation of the unitary translocation of a bonding defect. Thick lines represent water molecules forming hydrogen bonds (*dashed lines*) with each other and with the channel. (*Top*) A bonding defect is on the 2nd water molecule from the right; (*Middle*) reorientation of water 3 creates a hydrogen-bonding defect between water molecules 2 and 3; (*Bottom*) subsequent reorientation of water 2 moves the bonding defect to water 3.

three states, which results in the displacement of the bonding defect. This process, which occurs spontaneously in the simulations, is depicted schematically in Fig. 4. The conformations of the wire include metastable states in which one water molecule is a bonding defect, as well as transient conformations in which two adjacent water molecules are perpendicular to the channel axis. The unitary translocation of a bonding defect arises from the succession of two elementary reorientation steps. First, a water molecule adjacent to the bonding defect ($\mu_{zi\pm1} = 0$) reorients from a polarized state ($\mu_{zi} = \pm1$) to perpendicular ($\mu_{zi} = 0$). This process replaces one water-to-water H bond by a water-to-channel H bond, which creates a hydrogen-bonding defect, in a configuration which is sometimes referred to as negative Bjerrum defect, whereby two adjacent water O atoms are without an intervening H atom. Inversely, in the second step water $i \pm 1$ reorients from $\mu_{zi\pm1} = 0$ to ∓1, which eliminates the hydrogen-bonding defect in the wire and completes the unitary progression of the bonding defect. Thus, the hydrogen-bonding coordination provided by gA determines at once the nature of the bonding defect and the detailed mechanism for its migration (Pomès, 1999). It is the alternation of the two types of bonding defects that mediates the unitary migration of a bonding defect in the gA channel.

The dynamics of dipole reorientation of the pore water molecules is illustrated in Fig. 5. Initially, the 2nd water molecule from the bottom is a bonding defect (as depicted in Fig. 3). Sequences of reorientations trigger the migration

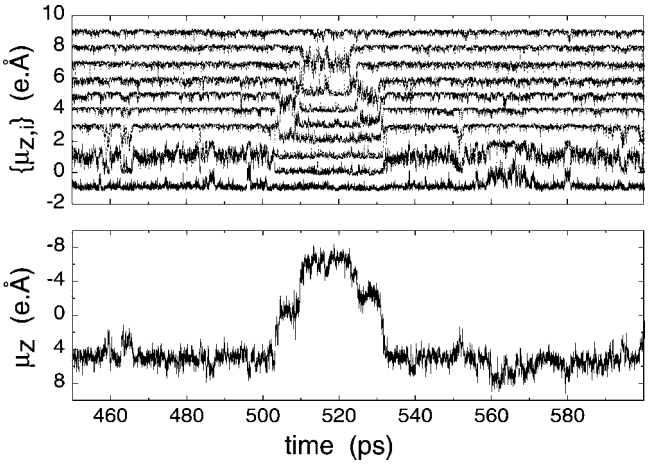

FIGURE 5 (*Top*) Time evolution of individual water dipole moment projections on the channel (z) axis obtained from molecular dynamics simulation of the unprotonated water wire. Each of the dipole components fluctuates in the range $-1 < \mu_{zi} < 1$ e·Å; each is shifted by $(i - 1)$ e·Å for clarity. (*Bottom*) z-component of the total dipole moment of the wire for the same time window.

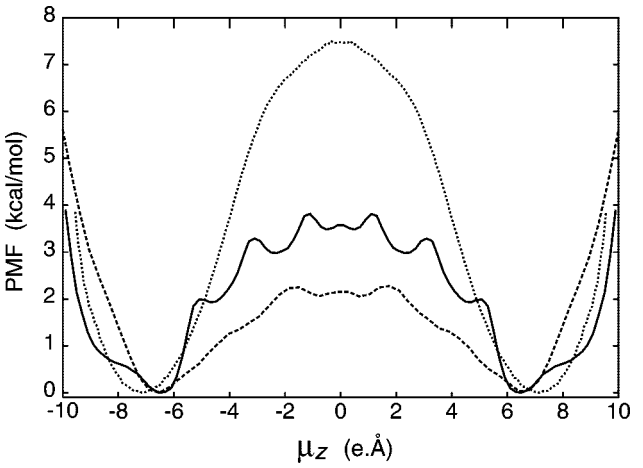

FIGURE 6 Potential of mean force for the reorientation of the unprotonated water chain in the single-file region of the GA channel: (*solid*) polarizable (PM6) water wire; (*dashed*) TIP3P water wire. Note that in the latter case, μ_z was scaled by 0.417, the partial charge of H atoms in the TIP3P model (Jorgensen et al., 1983), for direct comparison with the PM6 model, in which the formal charge of H atoms is 1. Results of the same calculation performed with nine PM6 water molecules in an analogous nonpolar channel (Pomès and Roux, 1998) are also shown (*dotted*) for comparison.

of the bonding defect between its two preferred locations, i.e., near the mouths of the pore. These transitions are infrequent and involve metastable states corresponding to bonding defects ($\mu_{zi} = 0$) located at water molecules 3 through 8. Thus, the bonding defect migrates from water 2 to water 5 at $t = 503$ ps, remains there for ~5 ps, and proceeds to water 8, which inverts the polarization of the chain. The reverse process takes place at $522 < t < 530$ ps, with intermediate stations at water molecules 7 and 6. The time evolution of the collective reaction coordinate for the translocation of the bonding defect, $\mu_z = \Sigma_i \mu_{zi}$, is depicted at the bottom of Fig. 5. The total dipole moment of the chain is highly sensitive to transitions in the orientation of individual water molecules and reflects the position of the bonding defect. The cooperativity of water reorientation was noted in earlier simulations (Chiu et al., 1989), and it was shown that the process is influenced by fluctuations in the conformation of the channel (Chiu et al., 1991). Although thermal fluctuations of the chain take the bonding defect (and the polarization of the chain) back and forth from end to end of the single file, this process is infrequent (it occurs only 12 times in the 20-ns simulation). This, together with cooperativity, suggests an energy-activated process.

PMF for the propagation of a bonding defect

The free energy profile for the translocation of a bonding defect, as calculated with umbrella sampling, is shown in Fig. 6. The results obtained for the two water models used, TIP3P and PM6, are qualitatively similar to each other. The preferred location of the bonding defect at water molecules 2 and 9 is reflected in the presence of a free energy well at $\mu_z = \pm 6.5$ e·Å, which corresponds to mostly-polarized conformations in which eight of the ten pore water molecules form an oriented hydrogen-bonded chain. The interconversion between these two polarized conformations involves an activation energy barrier centered at $\mu_z = 0$, which corresponds to a hydrogen-bonding defect located between water molecules 5 and 6 ($\mu_{z5} = \mu_{z6} = 0$). The barrier height is 3.8 kcal/mol with the polarizable water model PM6 and 2.2 kcal/mol with the TIP3P model. The PMF profile obtained from earlier simulations of a nonpolar channel of nine PM6 water molecules (Pomès and Roux, 1998), also shown in Fig. 6, is qualitatively similar but involves a much larger free energy barrier. At 7.6 kcal/mol, this barrier is about twice as large as that obtained for PM6 in the gA channel. Thus, the primary effect of the channel appears to be to catalyze the propagation of a bonding defect throughout the single file.

The PMF obtained with the PM6 model in gA includes six secondary minima located at $\mu_z = \pm 0.5$, ± 2.3, and ± 4.6 e·Å. Each of these secondary minima corresponds to metastable conformations in which one of the water molecules between water 2 and water 9 is in the process of flipping (see above). Similarly, the inflection points observed at $\mu_z = \pm 8.1$ e·Å correspond to conformations in which water molecules 1 and 10 are perpendicular to the channel axis. The PMF profile obtained with the TIP3P model also shows inflection points and secondary minima, albeit not as pronounced. By contrast, the PMF for reorientation of a wire in a nonpolar channel is much smoother, which is due to the absence of stabilizing interactions on the

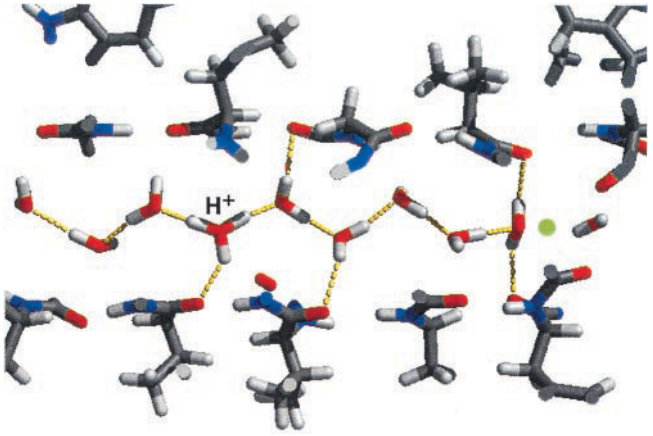

FIGURE 7 Representative structure of the hydrogen-bond network of a protonated water wire in gramicidin. In this snapshot, the excess proton (ionic defect) is in the form of a hydronium H_3O^+ and the bonding defect, highlighted by a green dot, is a hydrogen-bonding defect.

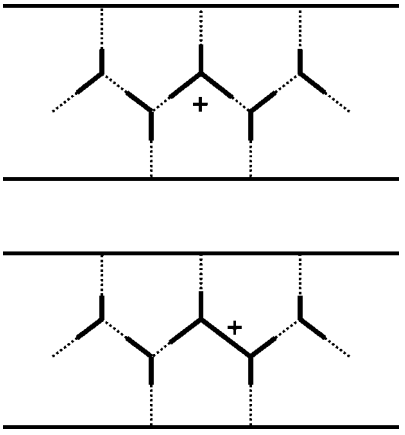

FIGURE 8 Schematic representation of the hydrogen-bonded network coordination of both (*top*) hydronium and (*bottom*) Zundel forms of protonated water molecules in the gA channel.

channel wall. These results suggest that the physical origin for catalysis of the turn step in the gA channel is identical to that which gives rise to a bonding defect: by accepting two hydrogen bonds from a water molecule, the carbonyl O atoms lining the pore interior stabilize intermediate arrangements of the water wire in which a water molecule is in the process of reorienting or flipping between its two preferred (polarized) states.

Protonated wire

Structure

A representative structure of the protonated water chain is shown in Fig. 7. The presence of the excess proton modifies the strength and the topology of water-water hydrogen bonds. As discussed in detail elsewhere (Pomès and Roux, 1995, 1996a,b), in a single-file environment the hydrated proton can generally be described either as a hydronium, OH_3^+, or as a "Zundel cation," $O_2H_5^+$, in which the proton is shared by two water molecules brought together by the excess charge in a strong hydrogen bond. At 2.4 Å, this strong hydrogen bond is much shorter than a typical water-water hydrogen bond (in the absence of an excess proton). In gA, as in nonpolar water-filled pores, the polarization of the water chain induced by the excess charge extends beyond the immediate vicinity of the ion. The excess proton is surrounded on either side by two oriented chains of water molecules pointing their O atom toward the positive charge.

By contrast to water-water interactions, the topology of the hydrogen-bonded network formed between water molecules and the channel is not affected significantly by the excess proton. In particular, protonated water molecules retain a hydrogen-bonding coordination of exactly three, as depicted in Fig. 7. In general, the hydrogen-bonded chain does not extend through the entire length of the single-file region of the channel. Instead, interruptions of the chain, or bonding defects, are observed sufficiently far from the excess proton (Pomès and Roux, 1996b). When the proton is near the middle of the wire (as in Fig. 7), these defects are located preferentially at either end of the single-file region, whereas when the excess proton is closer to one of the mouths, the defect is located near the other mouth.

Dynamic fluctuations

The rapid exchange of H^+ in the chain of water molecules in gA occurs spontaneously with thermal fluctuations at 300 K (Pomès and Roux, 1996b). As depicted schematically in Fig. 8, this exchange involves transitions between successive hydronium-like and Zundel-cation-like arrangements of the water molecules. Accordingly, the dynamic relay of H^+ in the proton wire may be easily followed either by monitoring at every snapshot of the simulation, which O atom is closest to three H nuclei (hydronium-like water molecule), or alternatively, by monitoring the position of the shortest OO separation (proton-sharing water dimer). These two reaction coordinates are complementary ways to view the translocation process (Pomès and Roux, 1996b). However, neither of these representations describes the translocation process fully, because they implicitly assume that hopping of the excess proton is entirely determined by the local arrangement of the one or two water molecule(s) closest to it. Rapid cascades in the movement of the hydrated proton over as many as six or seven water molecules were observed occasionally, suggesting that collective fluctuations are important to long-range transport (Pomès and Roux, 1996b).

Although the two steps of the Grotthuss mechanism are studied separately in the present work, it should be stressed that the propagation of H^+ is not independent of reorientation steps. The migration of bonding defects standing in the

path of H^+ is a prerequisite to complete proton translocation, because H^+ transfer necessitates preexisting and suitably-oriented hydrogen bonds. Thus, the slower rate of transport of bonding defects apparently limits the rate of translocation of the ionic defect in gA (Pomès and Roux, 1996b). Conversely, it might be expected that the entry of H^+ at one end of an unprotonated single file would hasten the translocation of the bonding defect via stabilization of one polarized conformation of the wire relative to the other. The polarization of water molecules induced by the presence of Na^+ at the entrance of the channel was noted in an earlier computational study of gA (Jordan, 1990).

The displacement of ionic and bonding defects occurs on different time scales. The migration of bonding defects is governed by water reorientation events that were observed to occur infrequently in the range of 100 ps or longer. This is significantly slower than the movement of H^+, which takes place in the picosecond or subpicosecond time range (Pomès and Roux, 1996b). For this reason, the average position of H^+ may remain in the vicinity of its starting point over simulations of a few hundred picoseconds. In the present work, successive simulations for which the excess proton was equilibrated at various positions were used to overcome the separation of time scales between ionic and bonding defect translocation. The collective reaction coordinate, μ_z, used in the present study reflects the polarization of the wire by taking into account not only the position of the excess proton but also the relative distribution of O and H nuclei along the channel axis z (Pomès and Roux, 1998). Thus, this reaction coordinate incorporates the presence of bonding defects in gA.

PMF for the propagation of an ionic defect

Because bonding defects move on a time scale comparable with that of the simulations, it is important that the ensemble of conformations used for the calculation of the PMF cover not only the displacement of H^+ but also of the bonding defect. This proved essential to the proper convergence of the PMF for the migration of an excess proton from end to end of the single-file region, which is shown in Fig. 9. This profile represents the reversible thermodynamic work for the complete translocation of the protonic defect. At $\mu_z = 0$, the center of charge is located on average near the center of the channel, whereas numerical values of $\mu_z \cong \pm 3$ e·Å correspond to configurations in which H^+ is located at the extremity of the polarized water chain with the ionic defect near $z = \pm 10$ Å and the total dipole moment of the wire pointing away at ∓ 7 Å. The largely activation-less PMF profile suggests a diffusive mechanism for proton hopping. The shallow well centered at the origin indicates that the excess proton is somewhat better "solvated" near the dimer junction with a moderate preference over outlying single-file locations reflected by a 1-kcal/mol drop in free energy. This could be due in part to the propensity of extremal water molecules to form bonding defects. A corollary to the polarization of water around the excess proton is that H^+ is always hosted by polarized water molecules, never by a bonding defect. In addition, finite-size effects could lead to an artificial bias in proton location. In studies of nonpolar channels without water caps, the excess proton remained localized near the center of the wire, whereas in the presence of droplets of 25 water molecules, H^+ was evenly distributed (Pomès and Roux, 1998). A similar effect was also observed in another study (Mei et al., 1998). In the present study, increasing the size of the caps from 36 to 64 water molecules each (results not shown) did not affect significantly the equilibrium distribution of H^+ in the single file. This indicates that the water caps used in the present study are adequately large and do not underlie the bias in proton location.

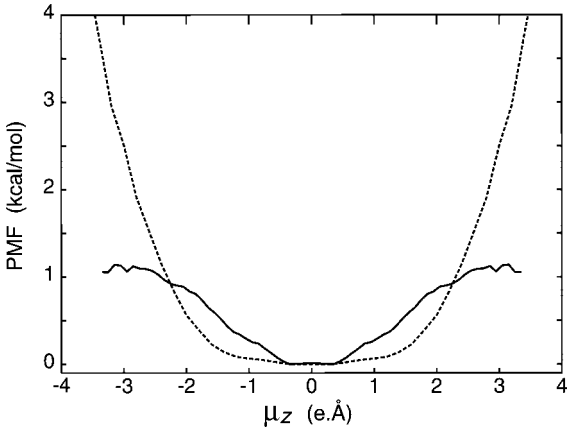

FIGURE 9 Potential of mean force for the translocation of an excess protonic charge (*solid line*) in the lumen of gramicidin and (*dashed line*) in an analogous, nonpolar channel (Pomès and Roux, 1998).

The PMF obtained for a nonpolar homolog of the channel (Pomès and Roux, 1998) is also depicted in Fig. 9. This profile, which was obtained in a very similar water system consisting of a single file of nine water molecule between spherical droplets of 25 water molecules each ("dumbbell" model), is a broad single well in the region $-2.0 < \mu_z < 2.0$ e·Å. This result indicates that in the absence of hydrogen-bonding partners to water molecules in the pore, no work is required to relay an excess proton from one end of the single file water chain to the other. This result is largely reproduced in gA, which suggests that the local environment provided by the channel is well suited for proton mobility. Thus, based on the present results it appears that the periodicity of groups presented by gramicidin provides no binding site or "trap" of protons in the single-file region.

Gramicidin as a proton duct

Our choice of molecular system reflects the focus of this work on the specific contributions made by the peptide on

proton conduction through a comparison of the molecular mechanisms obtained in nonpolar channels and in gA. This incremental, comparative approach presents the advantage of mitigating the effect of systematic errors inherent to empirical energy functions. Clearly, this approach also limits the scope of our conclusions. The absence of the lipid membrane precludes a realistic treatment of long-range electrostatic interactions, which play a role in the translocation of ions. Based on studies of proton permeation in which Trp residues were fluorinated and replaced by Phe residues, it has been proposed that dipole-dipole interactions between water molecules and indole rings could play a role in the preferred arrangement of water molecules in the channel, particularly near the mouths of the pore (Phillips et al., 1999). Our simplified representation of the bulk-water/channel interface makes the model inadequate to the treatment of such effects, as well as of the entrance and exit of protons and of water molecules.

The present results highlight the effect of water-water and water-channel hydrogen-bonding interactions at play in gA (Pomès and Roux, 1996b). The fine balance between these forces modulates the structure and dynamic fluctuations of the hydrogen-bonded network, which in turn govern the mechanisms of translocation of bonding and ionic defects in the single-file region of the channel. For a valid description of the mechanism it is therefore essential that the relative strengths of water-water and water-channel interactions be adequately modeled. Quantitative discrepancies in the activation energy for the reorientation of the water wire in gA (Fig. 6) obtained with PM6 and TIP3P reflect the different nature of these two water models. Despite this difference, the qualitative agreement obtained for the mechanism of translocation of a bonding defect indicates that both models, which exhibit identical mechanisms of reorientation in nonpolar channels (Pomès, 1999), also respond consistently to gA. In particular, the two models are in agreement regarding the coordination of water molecules, the nature of the bonding defect, and its preferred distribution in the unprotonated wire.

The relationship between water coordination and hop versus turn mobility in proton wires has been discussed elsewhere in a comparison of the Grotthuss mechanism in liquid water, in nonpolar channels, and in gA (Pomès, 1999). Implications of the molecular mechanism for the permeation of H^+ in nonpolar channels were proposed in terms of proton leakage via transient hydrogen-bonded chains (Pomès and Roux, 1998). In the absence of water-channel hydrogen-bonding interactions, each water molecule in the wire is tightly coordinated to both of its neighbors. As a result, there are no bonding defects in the chain and water molecules move in concert (i.e., cooperative motions of the O atoms are enhanced). Both of these effects conspire to the high mobility of H^+ in single-file arrays of water molecules embedded in nonpolar channels (Pomès and Roux, 1996b). However, the large activation energy calculated for the reorientation of water molecules (Pomès and Roux, 1998; Pomès, 1999) suggests that the turn step of the Grotthuss mechanism would be prohibitively long compared with the lifetime of single-file hydrogen-bonded arrays of water in a nonpolar cavity. Thus, transient water chains, which have been proposed to mediate the leakage of protons through pure lipid membranes (Nagle, 1987; Marrink et al., 1996; Paula et al., 1997) and to play a role in the uptake of H^+ in proton pumps (Wikström, 1998), would be suited at best to the passage of only one proton before breaking apart. In such a mechanism, the rate-limiting step for proton transport would be the nucleation of the wire.

By contrast to leakage, efficient proton-relaying channels such as gA provide a different mechanism for the rapid succession of proton conduction cycles. The analysis of this and previous simulation studies (Pomès and Roux, 1996b; Pomès, 1999) offers clues as to why gA constitutes a more effective proton duct than hypothetical hydrophobic counterparts. This is achieved by assisting the proton-relay chain in tackling the dual and seemingly contradictory requirement of a proton wire: to enable strong (water-water) hydrogen bonds between relaying groups for the rapid transfer and relay of H^+ and to help weaken (and break) these hydrogen bonds so as to facilitate the reorientation of proton-relaying groups.

Locally, ideal solvation of protons in aqueous systems is achieved by a coordination of three hydrogen-bond acceptors, because that is the coordination of protonated water molecules in OH_3^+ and $O_2H_5^+$ ions (Agmon, 1995). In the single-file region of gA, carbonyl O atoms of the peptide provide the extra hydrogen-bond acceptor that is missing in nonpolar channels (Fig. 8). Thus, the effect of gA on proton solvation (i.e., on the stabilization of an ionic defect) is similar to that observed above regarding the two forms of bonding defects (Fig. 4): the hydrogen-bond structure stabilizes both forms of the ionic defect (and by the same token, of larger protonated clusters of the form $O_nH_{2n+1}^+$ also found in gA). Furthermore, it is because both primary forms of the two types of defects are locally stabilized that the migration of ionic and bonding defects, whose elementary event consists of interconversions between these two forms (Figs. 4 and 8), is facilitated. In addition, mobility of protons benefits from the equivalence of proton-relay groups (i.e., the absence of proton-binding sites) in the pore. Thanks to the periodicity of the channel backbone and to the polarization and equal propensity of water molecules pointing left and right, protonic solvation is approximately as good anywhere along the single file. Likewise, the bonding defect is locally stabilized throughout the length of the pore. Thus, the hydrogen bond coordination offered by the gA channel achieves an effective compromise for the stabilization and the mobility of both ionic and bonding defects.

CONCLUSIONS AND PERSPECTIVES

We studied the complete translocations of a protonic defect and of a bonding defect by water molecules in the single-file region of the gA channel. We found that the mobility of an excess proton in gA is essentially determined by the fine structure and the dynamic fluctuations of the hydrogen-bonded network. The translocation of H^+ is mediated by spontaneous (thermal) fluctuations in the relative positions of oxygen atoms in the wire. In this diffusive mechanism, a shallow free-energy well slightly favors the presence of the excess proton near the middle of the channel. The unprotonated water chain adopts either one of two polarized conformations corresponding to oriented donor-acceptor hydrogen-bond pattern along the channel axis. Interconversion between these two conformations is an activated process that occurs via the sequential reorientation of water molecules of the wire. The effect of hydrogen bonding between channel and water on proton conduction was analyzed by comparison to the results obtained previously in a study of model nonpolar channels, in which such interactions were missing (Pomès and Roux, 1998). This analysis revealed that hydrogen-bond donation from water to the backbone carbonyl oxygen atoms lining the pore interior not only offers a compromise for the solvation and the mobility of an excess proton, it also enables the emergence of a bonding defect and facilitates its transport.

Among the challenges facing the study of biological ion transport mechanisms, particularly in the case of proton movement, are the difficulty to detect ion movement experimentally and to relate structure and function. The present study has opened the way to a better understanding of ion channel structure-function relationships by allowing the first confrontation of a molecular-level proton translocation mechanism with experimental measurements. Based on the results presented here, a framework model was developed for single-proton transport flux through gramicidin (Schumaker et al., 2000, 2001). That model describes the transport of H^+ (ionic defect) and of a bonding defect by potential of mean-force profiles (Figs. 6 and 9) and diffusion coefficients obtained from molecular dynamics simulations. Proton entrance and exit in and out of the single-file region, which were not studied by molecular dynamics in the present model, are represented parametrically. A reasonable choice of these parameters yields a good fit to experimental proton conductance data (Eisenman et al., 1980).

Theoretical approaches have begun to provide unprecedented and meaningful insight on the transient events governing proton relay mechanisms. Whereas the detailed studies performed to date on biological systems have been limited to the water chain embedded in the gramicidin channel, the results of these studies provide both a framework for understanding the basic physical principles at play in water wires and an impetus for the study of relay mechanisms in more complex proton wires. What is emerging from this and preceding studies of water wires is that the control of proton movement in biomolecular systems may be achieved with subtle local structural fluctuations of hydrogen bonded networks of low dimensionality, which are themselves determined by the fine hydrogen-bonding coordination, arrangement, and topology of proton-relay groups. The low dimensionality of a biological proton wire offers the possibility of a tight control of the geometry and the topology of hydrogen-bond interactions. The low-amplitude fluctuations of a flexible array (the proton wire) are thus mastered by a comparatively rigid environment presenting a few "judiciously disposed" hydrogen-bond partners.

Efficient proton conduction requires a wire that can alternatively form strong hydrogen bonds and break them relatively easily with thermal fluctuations. Water molecules are well suited for that, because water is ubiquitous in biological systems and forms highly modulable hydrogen-bonded networks. gA has harnessed those properties to assist both hop and turn steps of the Grotthuss mechanism. By the same token, it may be expected that somewhat similar features in the coordination of hydrogen-bond networks will be observed in other biomolecules that provide efficient ducts for the passive long-range relay of H^+. In particular, based on the present study the detailed characterization of the structure of hydrogen-bonded arrays of water molecules embedded in channels and enzyme cavities might offer a clue as to their ability to mediate rapid proton transport. Inversely, it is likely that other proteic matrices make use of the coordination properties (both static and dynamic) of water molecules and of other titratable groups to control the long-range transport of protons in other ways: for the selectivity, delay, gating, pumping, and blockage of protons.

Stimulating discussions with Samuel Cukierman, Mark Schumaker, and Ching-Hsing Yu are gratefully acknowledged. We also thank C.-H. Yu for his help in the preparation of Table 1. This work was supported by a grant from the Canadian Institutes of Health Research. R.P. is a CRCP Chairholder.

REFERENCES

Agmon, N. 1995. The Grotthuss mechanism. *Chem. Phys. Lett.* 244: 456–462.

Akeson, M., and D. W. Deamer. 1991. Proton conductance by the gramicidin water wire. *Biophys. J.* 60:101–109.

Arseniev, A. S., I. L. Barsukov, V. F. Bystrov, A. L. Lomize, and Y. A. Ovchinnikov. 1985. ^{1}H-NMR study of gramicidin-A transmembrane ion channel: head-to-head right handed single stranded helices. *FEBS Lett.* 186:168–174.

Brewer, M. L., U. W. Schmitt, and G. A. Voth. 2001. The formation and dynamics of proton wires in channel environments. *Biophys. J.* 80: 1691–1702.

Brooks, B. R., R. E. Bruccoleri, B. D. Olafson, D. J. States, S. Swaminathan, and M. Karplus. 1983. CHARMM: a program for macromolecular energy minimization and dynamics calculations. *J. Comput. Chem.* 4:187–217.

Chiu, S.-W., E. Jacobsson, S. Subramaniam, and J. A. McCammon. 1991. Time-correlation analysis of simulated water motion in flexible and rigid gramicidin channels. *Biophys. J.* 60:273–285.

Chiu, S.-W., S. Subramaniam, E. Jacobsson, and J. A. McCammon. 1989. Water and polypeptide conformations in the gramicidin channel. *Biophys. J.* 56:253–261.

Cukierman, S. 2000. Proton mobilities in water and in different stereoisomers of covalently linked gramicidin A channels. *Biophys. J.* 78: 1825–1834.

Decornez, H., K. Drukker, and S. Hammes-Schiffer. 1999. Solvation and hydrogen-bonding effects on proton wires. *J. Phys. Chem. A* 103: 2891–2898.

DeCoursey, T. E., and V. V. Cherny. 1999. An electrophysiological comparison of voltage-gated proton channels, other ion channels, and other proton channels. *Isr. J. Chem.* 39:409–418.

Dencher, N. A., H. J. Sass, and G. Büldt. 2000. Water and bacteriorhodopsin: structure, dynamics, and function. *Biochim. Biophys. Acta.* 1460:192–203.

Doyle, D. A., J. M. Cabral, R. A. Pfuetzner, A. Kuo, J. M. Gulbis, S. L. Cohen, B. T. Chait, and R. MacKinnon. 1998. The structure of the potassium channel: molecular basis of K^+ conduction and selectivity. *Science.* 280:69–77.

Drukker, K., S. W. de Leeuw, and S. Hammes-Schiffer. 1998. Proton transport along water chains in an electric field. *J. Chem. Phys.* 108: 6799–6808.

Eisenman, G., B. Enos, J. Hägglund, and D. Sandblom. 1980. Gramicidin A as an example of a single filing ionic channel. *Ann. N. Y. Acad. Sci.* 329:8–20.

Finkelstein, A. 1987. Water movement through lipid bilayers, pores, and plasma membranes. *In* Theory and Reality. John Wiley & Sons, New York.

Grotthuss, C. J. T. de. 1806. Mémoire sur la décompostion de l'eau et des corps qu'elle tient en dissolution à l'aide de l'électricité galvanique. *Ann. Chim.*58:54–74.

Humphrey, W., A. Dalke, and K. Schulten. 1996. VMD: visual molecular dynamics. *J. Mol. Graphics.* 14:33–38.

Jordan, P. C. 1990. Ion-water and ion-peptide correlations in a gramicidin-like channel. *Biophys. J.* 58:1133–1156.

Jorgensen, W. L., J. Chandrasekhar, J. D. Madura, R. W. Impey, and M. L. Klein. 1983. Comparison of simple potential functions for simulating liquid water. *J. Chem. Phys.* 79:926–935.

Kandori, H. 2000. Role of internal water molecules in bacteriorhodopsin. *Biochim. Biophys. Acta.* 1460:177–191.

Ketchem, R. R., B. Roux, and T. A. Cross. 1997. High resolution refinement of a solid-state NMR-derived structure of gramicidin A in a lipid bilayer environment. *Structure.* 5:11655–11669.

Knapp, E.-W., K. Schulten, and Z. Schulten. 1980. Proton conduction in linear hydrogen-bonded systems. *Chem. Phys.* 46:215–229.

Kumar, S., D. Bouzida, R. H. Swendsen, P. A. Kollman, and J. M. Rosenberg. 1992. The weighted histogram analysis method for free-energy calculations in biomolecules: I. The method. *J. Comp. Chem.* 13:1011–1021.

Lanyi, J. K. 1999. Bacteriorhodopsin. *Int. Rev. Cytol.* 187:161–202.

Lanyi, J. K. 2000. Molecular mechanism of ion transport in bacteriorhodopsin: insights from crystallographic, spectroscopic, kinetic, and mutational studies. *J. Phys. Chem. B.* 104:11441–11448.

Levitt, D. G., S. R. Elias, and J. M. Hautman. 1978. Number of water molecules coupled to the transport of sodium, potassium, and hydrogen ions via gramicidin, nonactin, or valinomycin. *Biochim. Biophys. Acta.* 512:436–451.

Luecke, H. 2000. Atomic resolution structures of bacteriorhodopsin photocycle intermediates: the role of discrete water molecules in the function of this light-driven ion pump. *Biochim. Biophys. Acta.* 1460: 133–156.

MacKerell, A. D., Jr., D. Bashford, M. Bellot, R. L. Dunbrack, J. D. Evanseck, M. J. Field, S. Fischer, J. Gao, H. Guo, S. Ha, D. Joseph-McCarthy, L. Kuchnir, K. Kuczera, F. T. K. Lau, C. Mattos, S. Michnick, T. Ngo, D. T. Nguyen, B. Prodhom, W. E. Reither, I. I. I., B. Roux, M. Schlenkrich, J. C. Smith, R. Stote, J. Straub, M. Watanabe, J. Wiórkiewicz-Kuczera, and M. Karplus. 1998. All-atom empirical potential for molecular modeling and dynamics studies of proteins. *J. Phys. Chem. B.* 102:3586–3616.

Marrink, S. J., F. Jähnig, and H. J. C. Berendsen. 1996. Proton transport across transient single-file water pores in a lipid membrane studied by molecular dynamics simulations. *Biophys. J.* 71:632–647.

Mei, H. S., M. E. Tuckerman, D. E. Sagnella, and M. E. Klein. 1998. Quantum nuclear *ab initio* molecular dynamics study of water wires. *J. Phys. Chem. B.* 102:10446–10458.

Mitchell, P. 1961. Coupling of phosphorylation to electron and proton transfer by a chemi-osmotic type of mechanism. *Nature.* 191:144–148.

Nagle, J. F. 1987. Theory of passive proton conductance in lipid bilayers. *J. Bioener. Biomemb.* 19:413–426.

Nagle, J. F., and H. J. Morowitz. 1978. Molecular mechanisms for proton transport in membranes. *Proc. Natl. Acad. Sci. U. S. A.* 75:298–302.

Okamura, M. Y., M. L. Paddock, M. S. Graige, and G. Feher. 2000. Proton and electron transfer in bacterial reaction centers. *Biophys. Biochim. Acta.* 1458:148–163.

Paula, S., G. Volkov, N. van Hoek, T. H. Haines, and D. W. Deamer. 1997. Permeation of protons, potassium ions, and small polar molecules through phospholipid bilayers as a function of membrane thickness. *Biophys. J.* 70:339–348.

Phillips, L. R., C. D. Cole, R. J. Hendershot, M. Cotten, T. A. Cross, and D. D. Busath. 1999. Noncontact dipole effects on channel permeation: III. Anomalous proton conductance effects in gramicidin. *Biophys. J.* 77:2492–2501.

Pomès, R. 1999. Theoretical studies of the Grotthuss mechanism in biological proton wires. *Isr. J. Chem.* 39:387–395.

Pomès, R., and B. Roux. 1995. Quantum effects on the structure and energy of a protonated linear chain of hydrogen-bonded water molecules. *Chem. Phys. Lett.* 234:416–424.

Pomès, R., and B. Roux. 1996a. Theoretical study of H^+ translocation along a model proton wire. *J. Phys. Chem.* 100:2519–2527.

Pomès, R., and B. Roux. 1996b. Structure and dynamics of a proton wire: a theoretical study of H^+ translocation along the single-file water chain in the gramicidin A channel. *Biophys. J.* 71:19–39.

Pomès, R., and B. Roux. 1998. Free energy profiles for H^+ conduction along hydrogen-bonded chains of water molecules. *Biophys. J.* 75: 33–40.

Quigley, E. P., P. Quigley, D. S. Crumrine, and S. Cukierman. 1999. The conduction of protons in different stereoisomers of dioxolane-linked gramicidin A channels. *Biophys. J.* 77:2479–2491.

Roux, B. 1995. The calculation of the potential of mean force using computer simulations. *Comp. Phys. Commun.* 91:275–282.

Roux, B., and M. Karplus. 1994. Molecular dynamics simulations of the gramicidin channel. *Annu. Rev. Biophys. Biomol. Struct.* 23:731–761.

Sadeghi, R. R., and H. P. Cheng. 1999. The dynamics of proton transfer in a water chain. *J. Chem. Phys.* 111:2086–2094.

Sagnella, D. E., K. Laasonen, and M. L. Klein. 1996. Ab initio molecular dynamics study of proton transfer in a polyglycine analog of the ion channel gramicidin A. *Biophys. J.* 71:1172–1178.

Saraste, M. 1999. Oxidative phosphorylation at the *fin de siècle. Science.* 283:1488–1493.

Schmitt, U. W., and G. A. Voth. 1999. The computer simulation of proton transport in water. *J. Chem. Phys.* 111:9361–9381.

Schumaker, M. F., R. Pomès, and B. Roux. 2000. A framework model for single proton conductance through gramicidin. *Biophys. J.* 79: 2840–2857.

Schumaker, M. F., R. Pomès, and B. Roux. 2001. A combined molecular dynamics and diffusion model of single proton conduction through gramicidin. *Biophys. J.* 80:12–30.

Sjogren, T., M. Svensson-Ek, J. Hajdu, and P. Brzezinski. 2000. Proton-coupled structural changes upon binding of carbon monoxide to cyto-

chrome cd(1): a combined flash photolysis and X-ray crystallography study. *Biochemistry.* 39:10967–10974.

Stillinger, F. H. 1979. Dynamics and ensemble averages for the polarization models of molecular interactions. *J. Chem. Phys.* 71:1647–1651.

Stillinger, F. H., and C. W. David. 1978. Polarization model for water and its ionic dissociation products. *J. Chem. Phys.* 69:1473–1484.

Tian, F., and T. A. Cross. 1999. Cation transport: an example of structural based selectivity. *J. Mol. Biol.* 285:1993–2003.

Tuckerman, M., K. Laasonen, M. Sprik, and M. Parrinello. 1995. *Ab initio* molecular dynamics simulation of the solvation and transport of H_3O^+ and OH^- ions in water. *J. Phys. Chem.* 99:5749–5752.

Vuillemier, R., and D. Borgis. 1998. Quantum dynamics of an excess proton in water using an empirical valence-bond Hamiltonian. *J. Phys. Chem.* 102:4261–4264.

Vuillemier, R., and D. Borgis. 1999. Transport and spectroscopy of the hydrated proton: a molecular dynamics study. *J. Chem. Phys.* 111: 4251–4266.

Weber, T. A., and F. H. Stillinger. 1982. Reactive collisions of $H3O^+$ and OH^- studied with the polarization model. *J. Phys. Chem.* 86: 1314–1318.

Wikström, M. 1998. Proton translocation by bacteriorhodopsin and heme-copper oxidases. *Curr. Opin. Struct. Biol.* 8:480–488.

Woolf, T. B., and B. Roux. 1994. Molecular dynamics simulations of the gramicidin channel in a phospholipid bilayer. *Proc. Natl. Acad. Sci. U. S. A.* 91:11631–11635.

Zaslavsky, D., and R. B. Gennis. 2000. Proton pumping by cytochrome oxidase: progress, problems and postulates. *Biochim. Biophys. Acta.* 1458:164–179.